

Bamboo Nanocomposite: Impact of Poly (Ethylene-alt-Maleic Anhydride) and Nanoclay on Physicochemical, Mechanical, and Thermal Properties

Muhammad Adamu,^{a,b,*} Md. Rezaur Rahman,^a and Sinin Hamdan^c

The effects of montmorillonite nanoclay and poly(ethylene-alt-maleic anhydride) *via* vacuum impregnation technique in relation to the physicochemical, mechanical, and thermal properties of bamboo-reinforced nanocomposites were investigated. The functional groups in the raw bamboo and nanocomposites were identified using Fourier transform infrared spectroscopy. X-ray diffraction plots showed the prominent peak intensity at a diffraction angle of 73° due to the transformation of the amorphous structure to a crystalline structure in the prepared nanocomposite. The morphologies of the raw bamboo and the nanocomposites were compared using scanning electron microscopy analysis. There was an increase in the modulus of elasticity from 7.82 to 19.0 GPa (143%) and a corresponding increase in the modulus of rupture from 68.7 to 121.5 MPa (77%) of the raw bamboo to the nanocomposites, respectively. This increase implied a high increase in the mechanical properties of the developed nanocomposite. Both results from the differential scanning calorimetry and thermogravimetric analysis showed appreciable improvements in the thermal properties of the developed nanocomposite.

Keywords: Bamboo; Nanocomposite; Impregnation technique; Mechanical strength

Contact information: a: Department of Chemical Engineering and Energy Sustainability, Faculty of Engineering, Universiti Malaysia Sarawak, 94300, Kota Samarahan, Sarawak, Malaysia. b: Nigerian National Petroleum Corporation, NNPC Corporate Headquarters, Abuja, Nigeria; c: Department of Mechanical and Manufacturing Engineering, Faculty of Engineering, Universiti Malaysia Sarawak, 94300, Kota Samarahan, Sarawak, Malaysia; *Corresponding author: pullogurin@gmail.com

INTRODUCTION

The application of nanotechnology for upgrading both structural and functional properties of synthetic polymers has emerged as a new area of research among material scientists and engineers (Olad 2011; Shahadat *et al.* 2015). Though the synthesis and application of nanotechnology for production of new composite materials are well-recognized, there is a need to mitigate the current challenge of having materials that are durable, sustainable, cost-effective, and environmentally friendly (Muhammad *et al.* 2019). Thus, there is considerable interest for the continuous search for low-cost reinforced composites using only biodegradables (Yates and Barlow 2013; Thakur *et al.* 2014; Lu *et al.* 2015; Varghese and Mittal 2018).

As the global economy grows, there is a proportional increase in the world's demand for wood (Bais *et al.* 2015). Present figures indicate that wood trade has exceeded 1.8 billion m³, with the Asia-Pacific countries accounting for approximately 24% of the global market (Buongiorno *et al.* 2011). This demand for high-quality wood has led to non-renewable removal of hard wood in many developing nations and has become a serious

concern, especially in Asia (Warman 2014). Many countries have taken measures to ban commercial logging, and this development has led to a sharp rise in the cost of natural wood products.

The choice of natural fibers, such as timber, to replace some of these materials has recently been explored (Saiful Islam *et al.* 2012; Zhu *et al.* 2016; Hossen *et al.* 2018). However, the mechanical properties are often not satisfactory. Bamboo fibers generally have been a preferred choice due to their potential for the manufacture of materials that can be recyclable, biodegradable, and highly sustainable, especially in the advent of findings that are a combination of the matrix and natural fibers would yield composites with high strength-to-weight ratios (Huda *et al.* 2012; Imbulana *et al.* 2013). Additionally, each component of the matrix can effectively be utilized for optimum properties as required in the formation of a composite (Loh *et al.* 2013; Gheith *et al.* 2019). It has been established that high-end quality and sustainable industrial products can be formed from bamboo that eases consumer choice and desirability (Nahar and Hasan 2013; Anokye *et al.* 2016). Similarly, as a result of high strength-to-weight ratio, bamboo fibers are often referred to as natural glass fiber, and it is arguably an attractive substitute to steel in applications requiring tensile loading (Jawaid and Abdul Khalil 2011; Karthik *et al.* 2017; Siddique *et al.* 2017).

Recently, the synthesis of polymer-layered silicate (PLS) nanocomposite has been of great importance due to its applications in industrial and scientific research for the production of value-added materials with highly improved physical and thermal properties (Ahmad and Kamke 2011; Shipp 2011).

Synthesized PLS nanocomposites have shown remarkable improvement with improved physical and mechanical properties as compared with conventional micro or macro composites. These properties include increased strength, reduced gas absorptivity and flammability, heat resistance, and rapid biodegradability, which are required for numerous engineering applications ranging from construction to household products (Biswas and Ray 2001; Ray *et al.* 2002; Thomas *et al.* 2012). These properties are re-engineered due to the dispersion of the polymer matrix of the bamboo material as a nanoscale inorganic filler, consequently leading to an active interfacial area that translates to superior properties compared to those of the original bulk polymer (Zhang *et al.* 2015; Wang and Chen 2017). Scientifically, the inorganic filler particles are reduced to nanoscale dimensions that directly impact their properties (Sasthryar *et al.* 2014).

The final properties of the nanocomposites thus formed generally depend on the nature and compositions of the inorganic filler as well as the microstructure and interfacial interactions of the bamboo microstructure (Yu *et al.* 2014; Liew *et al.* 2017). Therefore, the choice of a suitable inorganic filler that will effectively interact with and change the microstructure remarkably is an essential step for the production of a good nanocomposite material (Reddy 2014; Chen *et al.* 2017). It is reported that the clay nanofiller has remarkable physical and mechanical properties compared to conventional filler polymers, such as talc, glass fibers, carbon black, and calcium carbonate particle, and are usually referred to as microsize fillers (Thostenson *et al.* 2005). For example, the processability, mechanical properties, and lightness of the bamboo fiber can still be maintained when clay nanofibers are used, and this has made it a preferred choice in the polymer industry (Meng and Park 2013; Gheith *et al.* 2019).

Clay nanofiller possesses a well-layered structure that is characteristic of silicate minerals (Jonoobi *et al.* 2015; Silva *et al.* 2018). Among the various types of clay that have been used as nanofiller, montmorillonite is the most common due to its abundance and

because it contains alkali metal cations, with a high surface area, great swelling capacity, strong cation exchange, and excellent absorptive properties (Kaur and Kishore 2012). Many studies have been made on composite and polymer blends such as propylene ethylene (PE) (Duy Tran *et al.* 2013). However, most of these plastics become immiscible because of their difference in polarity. To mitigate this compatibility issue, numerous efforts have been deployed to modify either the polymer or the composite. Some compatibilizers that have been evaluated have resulted in weak and unsatisfactory mechanical properties (Liu *et al.* 2003). The lower mechanical properties were attributed to weak interaction between the compatibilizers and the composite (Luo *et al.* 2009). Recently, attention has focused on the use of polymers containing reactive groups such as maleic anhydride (Liu *et al.* 2003; Salleh *et al.* 2014). The anhydride groups react with the hydroxyl groups present in the composite with a resultant composite with chemical bonding, and thus create dispersion of the composite, enhanced interfacial adhesion, and subsequently improved mechanical properties.

There are several chemical and surface modification techniques, and these include salinization, acetylation, benzoylation, corona/cold plasma maleisation, peroxide, impregnation, enzymatic, or isocyanate (Muhammad *et al.* 2019). Thus, the main objective of this study is to develop a bamboo nanocomposite material and investigate the effect of poly(ethylene-alt-maleic anhydride) (PEA) compatibilizer and nanoclay on the physical, thermal, morphological, and mechanical properties of the developed nanocomposite. In the present study, poly(ethylene-alt-maleic anhydride) and nanoclay were used to improve the physicochemical, thermal, and mechanical properties of bamboo nanocomposite by impregnation under vacuum technique. The raw bamboo (RB) and nanocomposites have been characterized using Fourier transform infrared (FTIR), X-ray diffraction (XRD), and scanning electron microscopy (SEM) analyses. The thermal and mechanical properties were reported in this study.

EXPERIMENTAL

Materials and Methods

Samples preparation

The bamboo (*Gigantochloa scortechinii*) with an average age of 3 years was obtained from a forest in Kota Samarahan, Sarawak, Malaysia. Analytical grade chemicals, including poly(ethylene-alt-maleic anhydride) (PEA) (99% purity, Sigma-Aldrich, St. Louis, MO, USA), sodium hydroxide (Merck Schuchardt, Hohenbrunn, Germany), ethanol (95% purity, Braun HmbG, Kronberg, Germany), benzoyl peroxide, and nanoclay (Cloisite, BYK, Wesel, Germany) were also used. Ethanol was used as a solvent to dissolve the reagents, sodium hydroxide was used to adjust the pH of the medium for enhanced polymerization, and benzoyl peroxide was used as catalyst. The bamboo tree was cut to prepare the specimen for the impregnation experiment. Specimens having the following dimensions were prepared: 300 mm in length, thickness of 20 mm, and 20 mm width. The bamboo strips were placed in a forced air convection heater (Impact Test Equipment Ltd., Stevenston Ayrshire, Scotland) for five days at 70 °C for conditioning and drying. This reduced or eliminated the water present in the bamboo, which caused the size to shrink and get replaced by the polymer and nanoclay.

Preparation of nanocomposites

The oven-dried bamboo strips were immersed in a solution prepared by adding the different amounts of montmorillonite nanoclay (calosite), sodium hydroxide, 10 mg of PEA, and 10 mg of benzoyl peroxide dissolved in 500 mL of ethanol. The bamboo and the solution were then transferred into a vacuum chamber at different times of impregnation. The impregnated specimens in the vacuum chamber were then later removed. The surfaces were adequately cleaned with tissue paper, covered with aluminum foil, and placed into an oven operating at a temperature of 80 °C for 48 h, to allow for polymerization process in the bamboo fiber and cross-linkage of the nanoclay into the composite to obtain the nanocomposite before being unwrapped. Table 1 shows the amount of clay, chemicals, pH of the medium, and time used during the impregnation process. The scheme of the research is outlined in Fig. 1.

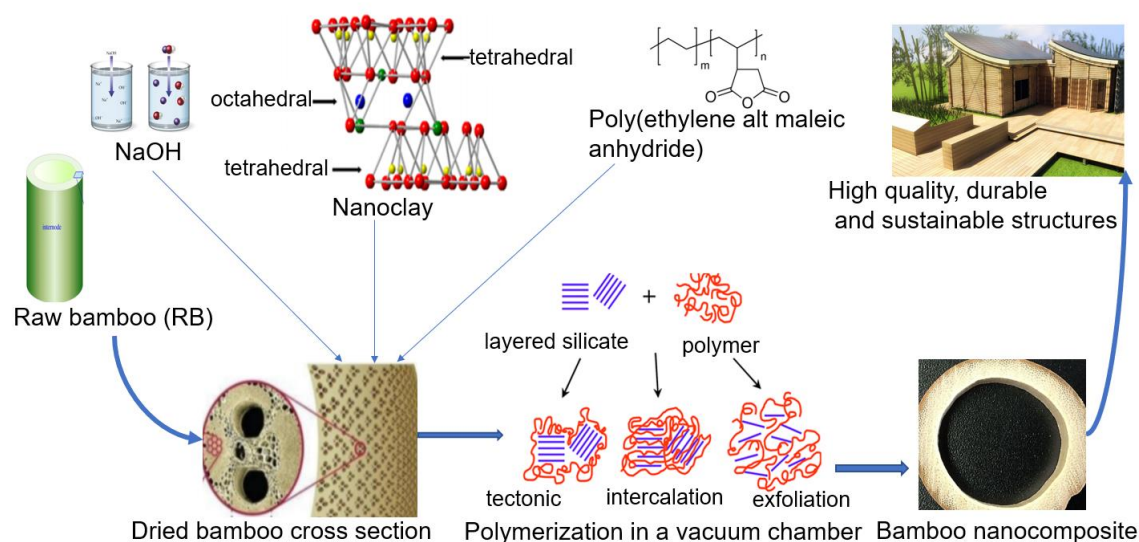


Fig. 1. Research scheme diagram

Table 1. Bamboo Impregnation at Different pH Levels

Experiment	Ethanol (mL)	PEA (g)	Benzoyl (mg)	Clay (g)	NaOH (g)	pH	Time (h)
PEA1	500	10	10	5	0	6	0.5
PEA2	500	10	10	10	0.5	7	1
PEA3	500	10	10	15	1	9	1.5
PEA4	500	10	10	20	1.5	10	2
PEA5	500	10	10	25	1.8	11	2.5

The impregnated bamboo was characterized by FTIR, XRD SEM, DSC, TGA, and a 3-point bending test.

Characterization

FTIR spectroscopy

The infrared spectra of all samples were obtained using a Shimadzu IRAffinity-1 spectrophotometer (Shimadzu, Kyoto, Japan). A wavenumber range from 4000 cm^{-1} to 600

cm^{-1} was used for the scan. This analytical tool is used in investigating polymers, clays, and clay minerals (Jonoobi *et al.* 2015).

X-ray diffraction

The structure and crystallinity of the RB and the prepared nanocomposites were characterized using XRD analysis. The pulverized specimen diffractograms were obtained using a Bruker D8 advanced X-ray diffractometer (Bruker Optik GmbH, Ettlingen, Germany) with $\text{CuK}\alpha$ radiation ($\lambda = 1.5418 \text{ \AA}$, rated as 1.6 kW).

SEM

The surfaces of the samples were imaged using a Hitachi TM3030 scanning electron microscope (JEOL, Ltd., Tokyo, Japan) supplied with a voltage of 20 kV in a vacuum. The surfaces of the samples were gold-coated (JEOL, Ltd., Tokyo, Japan) and imaged.

Mechanical Testing

Three-point bending test

This test was performed with a Shimadzu MSC-5/500 universal testing machine (Shimadzu, Kyoto, Japan) operating at a speed of 5 mm/min. The samples were in the dimensions of 300 mm (L) \times 20 mm (T) \times 20 mm (W) in accordance with ASTM D790-15e2 (2015) requirement of the machine. The modulus of rupture (MOR) and modulus of elasticity (MOE) for RB and TB samples were then calculated.

Thermal Testing

Differential scanning calorimetry (DSC)

The DSC measurements were conducted on a DSC Q10 (TA Instruments, New Castle, DE, USA) thermal system, in a sealed aluminium capsule. Each sample was weighed to approximately 3.5 mg to 4.0 mg and was heated at a rate of 10 $^{\circ}\text{C}/\text{min}$ and temperature from 35 $^{\circ}\text{C}$ to 450 $^{\circ}\text{C}$ (Rahman 2018). An average of three runs was reported for each set of samples.

Thermogravimetric analysis

Thermogravimetric analysis (TGA) was conducted using a TA Instruments 9222 thermal analyzer (TA Instruments, New Castle, DE, USA) with a platinum sample pan. The analysis was completed under nitrogen. Composites of 10 mg were analyzed at a maintained heating rate of 20 $^{\circ}\text{C}/\text{min}$ and heated to 600 $^{\circ}\text{C}$. Thermal solutions software (Universal Analysis 200, TA Instruments, version 5.5, New Castle, DE, USA) was used to transform the TG curve into the derivative thermogravimetric (DTG) curve.

RESULTS AND DISCUSSION

FTIR Analysis

From the FTIR study of the RB and nanocomposites shown in Fig. 2, the main functional groups, Al-OH and Si-O, were observed in the range of 1000 cm^{-1} to 500 cm^{-1} . The peak intensities between 667 cm^{-1} to 522.7 cm^{-1} and 1092 cm^{-1} to 1029 cm^{-1} resulted from the out-of-plane bending vibrations of $-\text{OH}$ groups and stretching vibrations of Al-O-Si of the clay in the bamboo (Li *et al.* 2006, 2013; Sharma *et al.* 2015; Ivashchenko *et*

al. 2016). Therefore, the strength of this band was higher for the nanocomposites than RB because of the bending vibrations of the AL-O-Si bond (Islam *et al.* 2015). The peaks between 4000 cm^{-1} to 3000 cm^{-1} showed broadening vibration of hydrogen bonds in $-\text{OH}$ groups, whereas the stretching of C-H in methylene and methyl groups occurred between 3000 cm^{-1} to 2900 cm^{-1} (Islam *et al.* 2015). The peaks in the vicinity of 1250 cm^{-1} corresponded to aromatic double bonds and thus higher intensity for treated nanocomposites compared to the RB. This change occurred due to the improved number of double bonds of the aromatics present in PEA (Lu *et al.* 2013).

The spectra of the nanocomposites showed a peak that had a low intensity above 3000 cm^{-1} , which matched to $-\text{OH}$ groups. The nanoclay displaced the free-bound water content of the bamboo matrix as it plasticized within the bamboo lumens (Liew *et al.* 2017). The change in peak intensities from 3426 cm^{-1} to 3396 cm^{-1} , 1091 cm^{-1} to 1029 cm^{-1} , and 667 cm^{-1} to 522.7 cm^{-1} showed that nanoclay was dispersed into the bamboo matrix (Hayati-Ashtiani 2012; Jagtap *et al.* 2016).

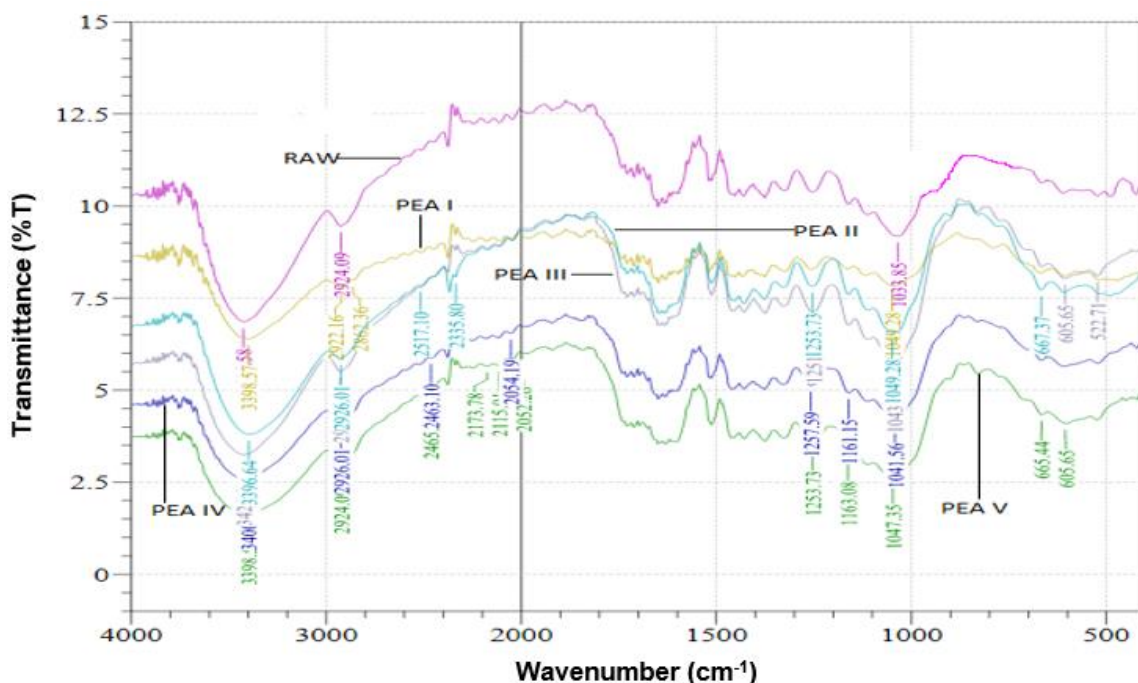


Fig. 2. FTIR spectra of RB and nanocomposites

XRD Analysis

X-ray diffraction is a useful tool for identifying the structure of the RB and that of the nanocomposites, which is presented in Fig. 3. The nanocomposite with PEA showed peaks at 2θ values of 23° , 43° , and 73° representing (001), (220), and (311) reflections, respectively (Venkatesan and Rajeswari 2017). The transformation occurred due to change in the structure of bamboo from an amorphous phase into a crystalline phase by the polymer matrix and nanoclay. The raw bamboo exhibited a peak at only angle 23° , which is the characteristic peak of amorphous bamboo. The XRD pattern of the nanocomposite indicated the intercalation and dispersion of polymer and clay into the bamboo, which resulted in the pronounced peaks.

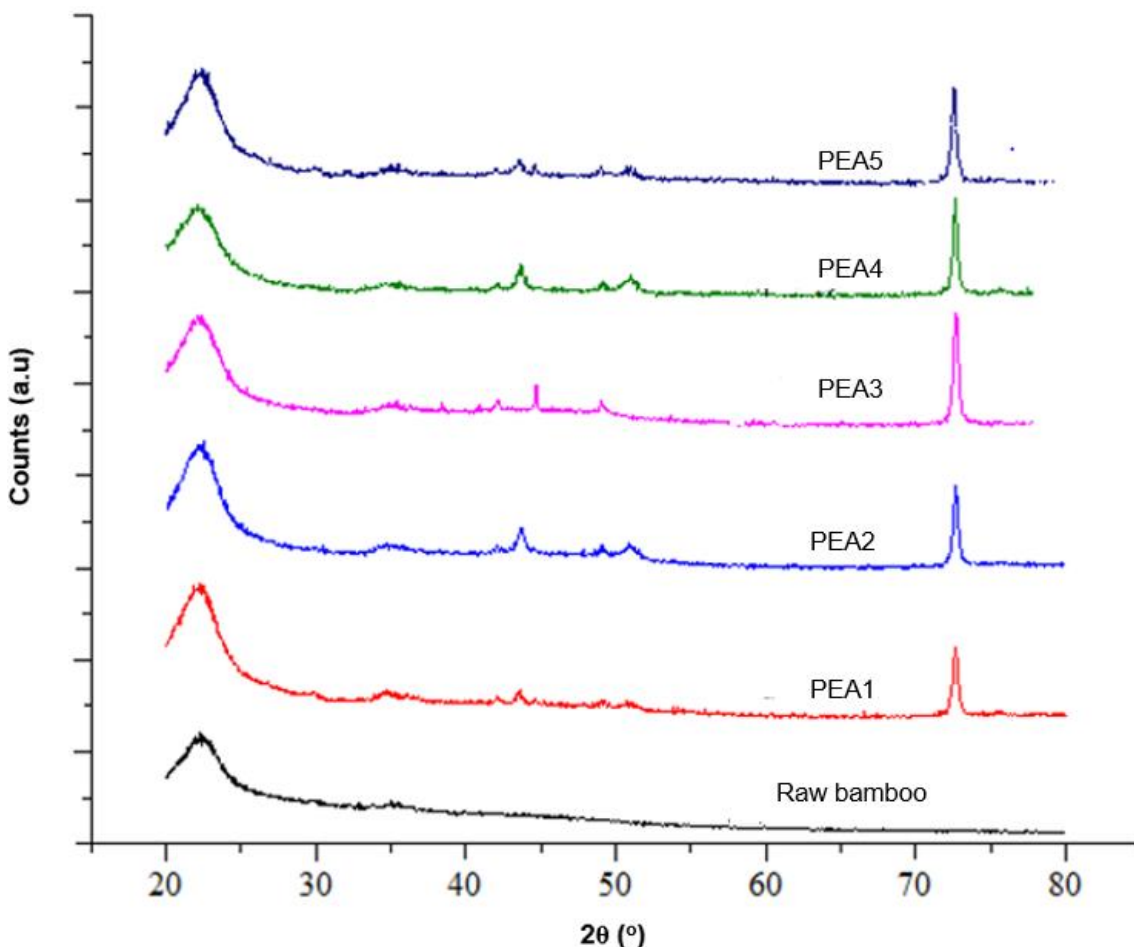


Fig. 3. XRD diffractograms of RB and PEA1, PEA2, PEA3, PEA4, and PEA5 nanocomposites

SEM Analysis

The SEM micrographs showed adhesion of polymer-filled lumens *via in-situ* polymerization and dispersion of nanoclay into the voids of the bamboo. In Fig. 4, for the nanocomposites (4b through 4f), the surfaces observed were smoother than the RB surface (Fig. 3a) that had visible pore spaces. This was a result of the role played by the polymer and nanoclay that acted as filler materials and filled the void spaces between the polymer and bamboo fiber pores (Xu *et al.* 2013).

Covalent bonds between the PEA and bamboo fiber walls were formed, which in turn filled the nanocomposites' void spaces when compared to the RB. A more rigid composite was formed as a result of this interaction, which showed compatibility and also translated into improved mechanical properties of the composite (Tao *et al.* 2016; Gheith *et al.* 2019). The compaction in the nanocomposites indicated that water could not easily flow into the bamboo. Thus, the treatment addressed hydrophobicity associated with bamboo and therefore extended its durability and external usage. The changes in morphology of both the RB and nanocomposites are illustrated in the SEM images in Fig. 4.

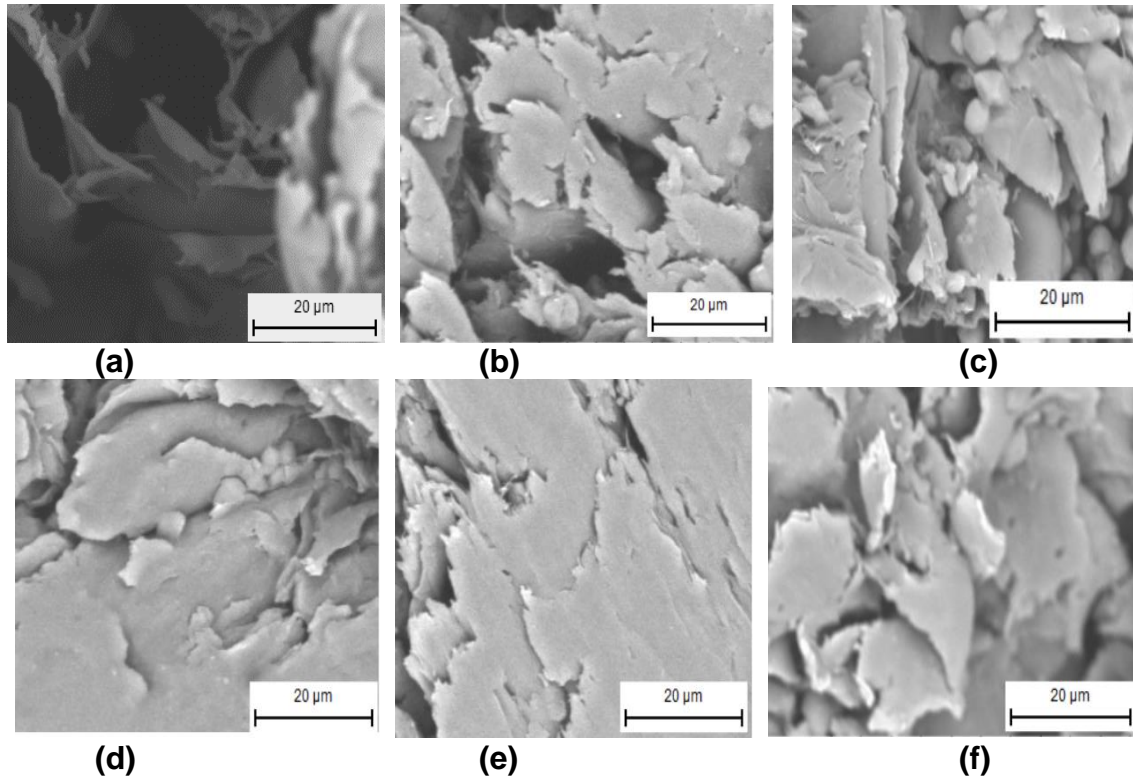


Fig. 4. SEM images (1500 \times) of: (a) raw bamboo, (b) PEA1, (c) PEA2, (d) PEA3, (e) PEA4, and (f) PEA5

Mechanical Properties

Table 2 shows that the values of MOE and MOR of the nanocomposites showed significant improvement compared to RB, with the highest values obtained in the PEA3 treatment. Modification of the RB indicated an approximate 143% increase in the elastic property when the bamboo was treated; this equally pointed out that it could withstand great loading pressure when used in construction applications. The treated bamboo additionally showed an increase of approximately 77% in its MOR, which was higher than similar materials like wood and timber.

Table 2. t-Test Study of MOE and MOR of RB and Nanocomposites

Samples	MOE (GPa)	t-Test Grouping 1	MOR (MPa)	t-Test Grouping 2
Raw Bamboo	7.82 ± 2.04	A	68.67 ± 27.29	D
PEA1	14.97 ± 3.02	B	102.10 ± 7.32	E
PEA2	14.57 ± 3.52	B	90.85 ± 10.27	D
PEA3	18.96 ± 3.09	D	121.48 ± 8.54	F
PEA4	11.20 ± 3.47	C	87.39 ± 22.15	D
PEA5	12.66 ± 2.20	C	96.18 ± 12.54	E

Same letters indicate non-significant difference at $\alpha = 5$; values represent means of 10 replicates while \pm values represent one standard deviation

Therefore, the nanoclay and polymer used were dispersed into the voids of the bamboo and improved its mechanical properties.

DSC Analysis

The DSC curves of the RB and formed nanocomposites are presented in Fig. 5. The figure indicates that RB exhibited three markedly separated endothermic peaks at 80 °C to 110 °C, 180 °C to 220 °C, and 330 °C to 400 °C, which corresponded to amorphous, para-crystalline, and crystalline phases, respectively (Mahato *et al.* 2013; Mattos *et al.* 2015). The para-crystalline parts and the amorphous sections were more susceptible to heat and chemicals than those of the crystalline components. The molecular movement of its non-crystalline phase was higher compared to the crystalline part (Bao *et al.* 2003; Rahman 2018). The movement of the chain of macromolecules was firm. This change in the movement was ascribed to the intramolecular forces present as well as intermolecular hydrogen bonding (Rahman *et al.* 2010). The first endothermic peak corresponded to the removal of absorbed water from the amorphous RB and the nanocomposites. The area of the peak of the nanocomposites was smaller than that of RB, which was due to the filler in the TB that inhibited the amorphous change and thereby reduced the amount of water absorbed into the RB. The hydrophobicity of the nanocomposites would be higher than that of the RB because of the ionic characteristics of nanoclay that made the water molecule to be tightly held together. The thermal stability of the second endothermic para-crystalline phase of the RB and nanocomposites was similar, whereas the para-crystalline enthalpy of RB was higher than that of the nanocomposites. The clay had no covalent bond with the bamboo but restricted the para-crystalline movement and thereby increased the crystallinity of the composite. The composite PEA3 showed higher para-crystalline enthalpy among all other treatments.

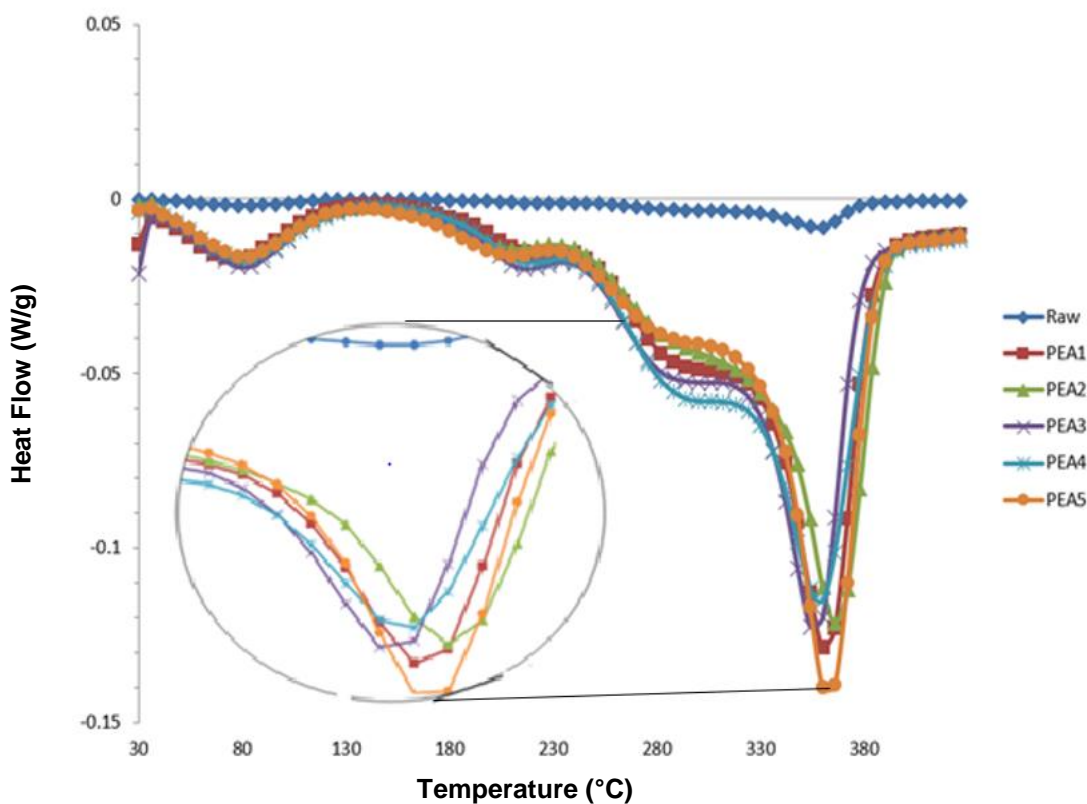


Fig. 5. DSC thermogram of (a) RB, (b) PEA1, (c) PEA2, (d) PEA3, (e) PEA4, and (f) PEA5

The molecule formed an induced dipole bond with the aromatic groups in the bamboo. It then converted the amorphous structure of bamboo to a para-crystalline structure. The para-crystalline endothermic enthalpy of the nanocomposites was lower than RB because PEA and clay entered the para-crystalline region of the bamboo to convert it into a crystalline region (Phetkaew *et al.* 2009). The nanoclay particle entered the amorphous region and restricted the amorphous movement of the molecule. The crystallinity of the nanocomposites was higher compared to the RB. Thus, the composites absorbed more heat than the raw bamboo.

Thermogravimetric Analysis

Figure 6 shows that the RB and nanocomposites had three stages of thermal decomposition and degradation. Stage 1 showed that the weight loss of all samples occurred at 72 °C and was a result of the evaporation of the absorbed moisture (Liu *et al.* 2013; Rahman 2018). Below 110 °C, the initial weight loss of the samples was lowest for PEA5, followed by PEA4, PEA2, PEA3, PEA1, and RB, which was a result of the hydrolyzed reaction with the –OH groups of bamboo wall as well as the surface modified clay filler that also filled the cavities of the formed nanocomposites.

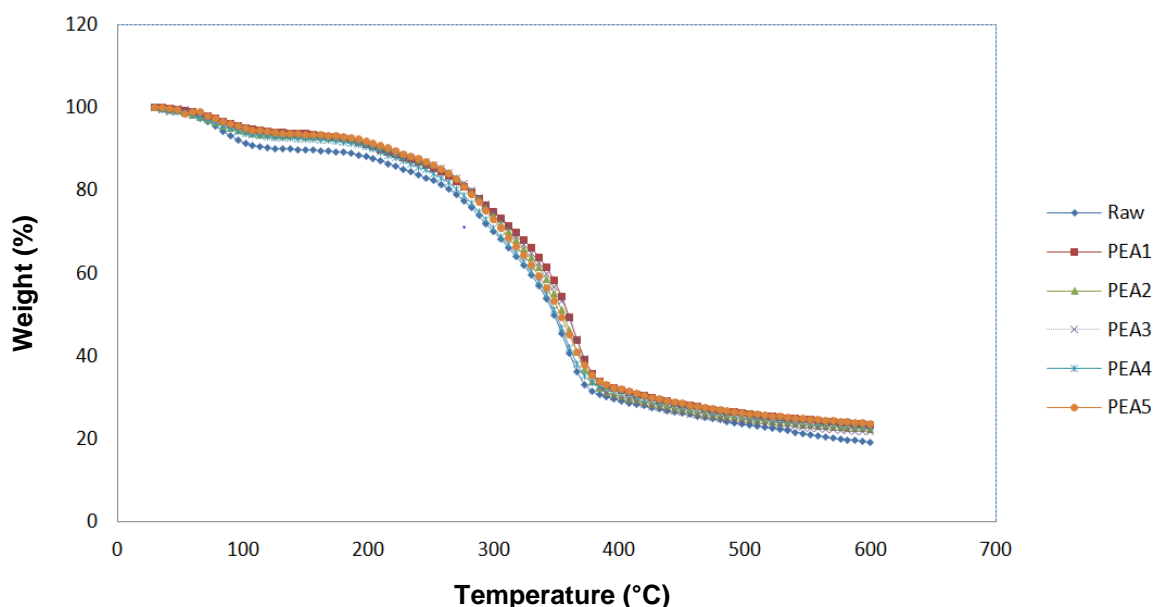


Fig. 6. TGA of (a) RB, (b) PEA1, (c) PEA2, (d) PEA3, (e) PEA4, and (f) PEA5

The second stage of thermal decomposition in the samples occurred at 125 °C, with an appreciable difference between the RB and nanocomposites at 250 °C due to the strong covalent bonds in the nanocomposite samples, which made weight loss noticeably lower in the nanocomposite samples compared to the RB similar to the second stage. The third stage of thermal decomposition, which occurred at 385 °C, additionally revealed an appreciable difference between the RB and nanocomposite samples, with decomposition being lower in the nanocomposites compared to the RB. This occurrence could be attributed to well-distributed clay layers blocking the way of unstable decomposition products throughout the composites during thermal degradation, and thus the remarkable improvement in thermal stability for nanocomposites formed during the third stage of

decomposition (García *et al.* 2009; Sánchez-Jiménez *et al.* 2012). Thermal properties of all samples are presented in Table 3.

Table 3. Result of TGA for RB and Composites

Sample	No. of Transition	Transition Temperature (°C)			Weight Loss Temperature (%)	Residual Weight (%) at Final Stage Transition
		T_i	T_m	T_f		
RAW	1	35.80	60.24	101.54	6.20	17.83
	2	117.21	146.35	169.70	44.71	
	3	176.58	354.51	578.59	31.26	
PEA1	1	41.42	78.36	127.26	5.62	22.69
	2	273.65	354.05	382.72	42.75	
	3	390.14	429.87	508.14	28.94	
PEA2	1	41.46	79.36	129.16	5.44	24.81
	2	274.24	351.20	381.98	41.02	
	3	390.65	428.48	507.85	28.73	
PEA3	1	42.01	77.35	127.02	5.57	23.30
	2	273.65	351.22	383.00	43.05	
	3	389.76	429.09	506.92	28.08	
PEA4	1	43.12	80.21	133.46	5.43	25.91
	2	273.11	352.42	382.07	40.69	
	3	389.71	429.06	506.24	27.97	
PEA5	1	41.39	80.02	128.22	5.24	24.94
	2	274.01	353.11	380.24	41.34	
	3	390.13	427.58	503.49	28.48	

T_i is initial temperature, T_m is temperature at which the rate of weight loss was maximum, and T_f is the final temperature

CONCLUSIONS

Bamboo nanocomposites were successfully prepared by cloisite Na⁺ clay and PEA, with the aim of improving properties of the bamboo as summarized below:

1. The nanocomposites demonstrated higher MOE and MOR than the raw bamboo. It was observed that through incorporation of 15 g of nanoclay and 10 mg of PEA at a pH of 9, the modified bamboo had an increase of 143% MOE and 77% MOR.
2. The SEM study revealed the presence of nanoclay in the lumen, void spaces, and cell wall of the bamboo, improving adhesion between the polymer and the bamboo; hence, it may reduce hydrophobicity.
3. The TGA and DSC analyses showed improved thermal stability of the nanocomposites compared to the raw bamboo. The improvement in thermal properties of the modified bamboo was attributed to good dispersion of the nanoclay and PEA polymer matrix into the bamboo.

4. There was modification of the composition and form of the raw bamboo as shown by XRD and FTIR, which resulted in improved mechanical properties of the prepared nanocomposites.

ACKNOWLEDGMENTS

Special thanks to the Department of Chemical Engineering and Energy Sustainability, Faculty of Engineering at the Universiti Malaysia Sarawak (UNIMAS) for supporting this research with Grant No. F02/SPGS/1443/2016/25.

REFERENCES CITED

- Ahmad, M., and Kamke, F. A. (2011). "Properties of parallel strand lumber from Calcutta bamboo (*Dendrocalamus strictus*)," *Wood Sci. Technol.* 45(1), 63-72. DOI: 10.1007/s00226-010-0308-8
- Anokye, R., Bakar, E. S., Jegatheswaran, R., and Awang, K. B. (2016). "Bamboo properties and suitability as a replacement for wood," *Pertanika Journal of Scholarly Research Reviews* 2(1), 64-80. DOI: 10.13140/RG.2.1.1939.3048
- ASTM D790-15e2 (2015). "Standard test methods for flexural properties of unreinforced and reinforced plastics and electrical insulating materials," ASTM International, West Conshohocken, PA, USA.
- Bais, A. L. S., Lauk, C., Kastner, T., and Erb, K. (2015). "Global patterns and trends of wood harvest and use between 1990 and 2010," *Ecol. Econ.* 119, 326-337. DOI: 10.1016/j.ecolecon.2015.09.011
- Bao, S. C., Daunch, W. A., Sun, Y. H., Rinaldi, P. L., Marcinko, J. J., and Phanopoulos, C. (2003). "Solid state two-dimensional NMR studies of polymeric diphenylmethane diisocyanate (PMDI) reaction in wood," *Forest Prod. J.* 53(6), 63-71.
- Biswas, M., and Ray, S. S. (2001). "Recent progress in synthesis and evaluation of polymer-montmorillonite nanocomposites," in: *New Polymerization Techniques and Synthetic Methodologies*, Springer-Verlag, Berlin, Germany, pp. 167-221. DOI: 10.1007/3-540-44473-4_3
- Buongiorno, J., Raunikar, R., and Zhu, S. (2011). "Consequences of increasing bioenergy demand on wood and forests: An application of the Global Forest Products Model," *J. Forest Econ.* 17(2), 214-229. DOI: 10.1016/j.jfe.2011.02.008
- Chen, H., Yu, Y., Zhong, T., Wu, Y., Li, Y., Wu, Z., and Fei, B. (2017). "Effect of alkali treatment on microstructure and mechanical properties of individual bamboo fibers," *Cellulose* 24(1), 333-347. DOI: 10.1007/s10570-016-1116-6
- Duy Tran, T., Dang Nguyen, M., Ha Thuc, C. N., Ha Thuc, H., and Dang Tan, T. (2013). "Study of mechanical properties of composite material based on polypropylene and Vietnamese rice husk filler," *J. Chem.* 2013, Article ID 752924. DOI: 10.1155/2013/752924
- García, M., Hidalgo, J., Garmendia, I., and García-Jaca, J. (2009). "Wood-plastics composites with better fire retardancy and durability performance," *Compos. Part A-Appl. S.* 40(11), 1772-1776. DOI: 10.1016/j.compositesa.2009.08.010
- Gheith, M. H., Aziz, M. A., Ghorri, W., Saba, N., Asim, M., Jawaid, M., and Alothman, O. Y. (2019). "Flexural, thermal and dynamic mechanical properties of date palm

- fibres reinforced epoxy composites," *J. Mater. Res. Technol.* 8(1), 853-860. DOI: 10.1016/j.jmrt.2018.06.013
- Hayati-Ashtiani, M. (2012). "Use of FTIR spectroscopy in the characterization of natural and treated nanostructured bentonites (montmorillonites)," *Part. Sci. Technol.* 30(6), 553-564. DOI: 10.1080/02726351.2011.615895
- Hossen, M. F., Hamdan, S., and Rahman, M. R. (2018). "Improved mechanical properties of silane treated jute/polyethylene/clay nanocomposites," *Malays. Appl. Biol.* 47(1), 209-216.
- Huda, S., Reddy, N., and Yang, Y. (2012). "Ultra-light-weight composites from bamboo strips and polypropylene web with exceptional flexural properties," *Compos. Part B-Eng.* 43(3), 1658-1664. DOI: 10.1016/j.compositesb.2012.01.017
- Imbulana, P. K., Fernandez, T., Jayawardene, P. A. R. P., Levangama, T. P., Perera, Y. K., Arachchi, H. N. K., and Mallawaarachchi, R. S. (2013). "Bamboo as a low cost and green alternative for reinforcement in light weight concrete," in: *SAITM Research Symposium on Engineering Advancements 2013 (SAITM – RSEA 2013)*, Malabe, Sri Lanka, pp. 166-172.
- Islam, M. S., Kovalcik, A., Hasan, M., and Thakur, V. K. (2015). "Natural fiber reinforced polymer composites," *Int. J. Polym. Sci.* 2015, Article ID 813568. DOI: 10.1155/2015/813568
- Ivashchenko, O., Jurga-Stopa, J., Coy, E., Peplinska, B., Pietralik, Z., and Jurga, S. (2016). "Fourier transform infrared and Raman spectroscopy studies on magnetite/Ag/antibiotic nanocomposites," *Appl. Surf. Sci.* 364, 400-409. DOI: 10.1016/j.apsusc.2015.12.149
- Jagtap, S. B., Mohan, M. S., and Shukla, P. G. (2016). "Improved performance of microcapsules with polymer nanocomposite wall: Preparation and characterization," *Polymer* 83, 27-33. DOI: 10.1016/j.polymer.2015.12.011
- Jawaid, M., and Abdul Khalil, H. P. S. (2011). "Cellulosic/synthetic fibre reinforced polymer hybrid composites: A review," *Carbohydr. Polym.* 86(1), 1-18. DOI: 10.1016/j.carbpol.2011.04.043
- Jonoobi, M., Oladi, R., Davoudpour, Y., Oksman, K., Dufresne, A., Hamzeh, Y., and Davoodi, R. (2015). "Different preparation methods and properties of nanostructured cellulose from various natural resources and residues: A review," *Cellulose* 22(2), 935-969. DOI: 10.1007/s10570-015-0551-0
- Karthik, S., Rao, P. R. M., and Awoyera, P. O. (2017). "Strength properties of bamboo and steel reinforced concrete containing manufactured sand and mineral admixtures," *Journal of King Saud University- Engineering Sciences* 29(4), 400-406. DOI: 10.1016/j.jksues.2016.12.003
- Kaur, N., and Kishore, D. (2012). "Montmorillonite: An efficient, heterogeneous and green catalyst for organic synthesis," *J. Chem. Pharm. Res.* 4(2), 991-1015.
- Li, F., Zhou, S., You, B., and Wu, L. (2006). "Kinetic investigations on the UV-induced photopolymerization of nanocomposites by FTIR spectroscopy," *J. Appl. Polym. Sci.* 99(4), 1429-1436. DOI: 10.1002/app.22629
- Li, L., Liu, G., Zhang, C.-Y., Ou, Q.-H., Zhang, L., and Zhao, X.-X. (2013). "Discrimination of bamboo using FTIR spectroscopy and statistical analysis," *Spectrosc. Spectral Anal. (Beijing, China)* 33(12), 3221-3225. DOI: 10.3964/j.issn.1000-0593(2013)12-3221-05
- Liew, F. K., Hamdan, S., Rahman, M. R., Mahmood, M. R., and Lai, J. C. H. (2017). "The effects of nanoclay and tin(IV) oxide nanopowder on morphological, thermo-

- mechanical properties of hexamethylene diisocyanate treated jute/bamboo/polyethylene hybrid composites," *J. Vinyl Addit. Technol.* 24(4), 358-366. DOI: 10.1002/vnl.21600
- Liew, F. K., Hamdan, S., Rahman, M. R., and Rusop, M. (2017). "Thermomechanical properties of jute/bamboo cellulose composite and its hybrid composites: The effects of treatment and fiber loading," *Adv. Mater. Sci. Eng.* 2017, Article ID 8630749. DOI: 10.1155/2017/8630749
- Liu, W., Wang, Y.-J., and Sun, Z. (2003). "Effects of polyethylene-grafted maleic anhydride (PE-g-MA) on thermal properties, morphology, and tensile properties of low-density polyethylene (LDPE) and corn starch blends," *J. Appl. Polym. Sci.* 88(13), 2904-2911. DOI: 10.1002/app.11965
- Liu, Z., Jiang, Z., Fei, B., and Liu, X. (2013). "Thermal decomposition characteristics of Chinese fir," *BioResources* 8(4), 5014-5024. DOI: 10.15376/biores.8.4.5014-5024
- Loh, Y. R., Sujana, D., Rahman, M. E., and Das, C. A. (2013). "Sugarcane bagasse – The future composite material: A literature review," *Resources, Conservation and Recycling* 75, 14-22. DOI: 10.1016/j.resconrec.2013.03.002
- Lu, N., Oza, S., and Tajabadi, M. G. (2015). "Surface modification of natural fibers for reinforcement in polymeric composites," in: *Surface Modification of Biopolymers*, V. K. Thakur, A. S. Singha (eds.), John Wiley & Sons, Hoboken, NJ, USA, pp. 224-237. DOI: 10.1002/9781119044901.ch9
- Lu, T., Jiang, M., Jiang, Z., Hui, D., Wang, Z., and Zhou, Z. (2013). "Effect of surface modification of bamboo cellulose fibers on mechanical properties of cellulose/epoxy composites," *Compos. Part B- Eng.* 51, 28-34. DOI: 10.1016/j.compositesb.2013.02.031
- Luo, F., Ning, N., Chen, L., Su, R., Cao, J., Zhang, Q., Fu, Q., and Zhao, S. (2009). "Effects of compatibilizers on the mechanical properties of low density polyethylene/lignin blends," *Chin. J. Polym. Sci.* 27(6), 833-842. DOI: 10.1142/s0256767909004552
- Mahato, D. N., Mathur, B. K., and Bhattacharjee, S. (2013). "DSC and IR methods for determination of accessibility of cellulosic coir fibre and thermal degradation under mercerization," *Indian J. Fibre Text. Res.* 38(1), 96-100.
- Mattos, B. D., De Cademartori, P. H. G., Missio, A. L., Gatto, D. A., and Magalhães, W. L. E. (2015). "Wood-polymer composites prepared by free radical *in situ* polymerization of methacrylate monomers into fast-growing pinewood," *Wood Sci. Technol.* 49(6), 1281-1294. DOI: 10.1007/s00226-015-0761-5
- Meng, L.-Y., and Park, S.-J. (2013). "Influence of carbon nanofibers on electrochemical properties of carbon nanofibers/glass fibers composites," *Curr. Appl. Phys.* 13(4), 640-644. DOI: 10.1016/j.cap.2012.10.008
- Muhammad, A., Rahman, M. R., Hamdan, S., and Sanaullah, K. (2019). "Recent developments in bamboo fiber-based composites: A review," *Polymer Bulletin* 76(5), 2655-2682. DOI: 10.1007/s00289-018-2493-9
- Nahar, S., and Hasan, M. (2013). "Effect of chemical composition, anatomy and cell wall structure on tensile properties of bamboo fiber," *Eng. J.* 17(1), 61-68. DOI: 10.4186/ej.2013.17.1.61
- Olad, A. (2011). "Polymer/clay nanocomposites," in: *Advances in Diverse Industrial Applications of Nanocomposites*, B. Reddy (ed.), InTechOpen, London, United Kingdom, pp. 113-138. DOI: 10.5772/14464
- Phetkaew, W., Kyokong, B., Khongtong, S., and Mekanawakul, M. (2009). "Effect of

- pre-treatment and heat treatment on tensile and thermal behavior of Parawood strands," *Songklanakarin Journal of Science and Technology* 31(3), 323-330.
- Rahman, M. R. (2018). *Wood Polymer Nanocomposites*, M. Rezaur Rahman (ed.), Springer, Cham, Switzerland. DOI: 10.1007/978-3-319-65735-6
- Rahman, M. R., Islam, M. N., and Huque, M. M. (2010). "Influence of fiber treatment on the mechanical and morphological properties of sawdust reinforced polypropylene composites," *J. Polym. Environ.* 18(3), 443-450. DOI: 10.1007/s10924-010-0230-z
- Ray, S. S., Yamada, K., Okamoto, M., and Ueda, K. (2002). "Polylactide-layered silicate nanocomposite: A novel biodegradable material," *Nano Lett.* 2(10), 1093-1096. DOI: 10.1021/nl0202152
- Reddy, K. R. (2014). "Polypropylene clay nanocomposites," in: *Handbook of Polymernanocomposites. Processing, Performance and Application: Volume A: Layered Silicates*, J. K. Pandey, K. R. Reddy, A. K. Mohanty, and M. Misra (eds.), Springer-Verlag Berlin-Heidelberg, Berlin, Germany, pp. 153-175. DOI: 10.1007/978-3-642-38649-7_2
- Saiful Islam, M., Hamdan, S., Jusoh, I., Rezaur Rahman, M., and Ahmed, A. S. (2012). "The effect of alkali pretreatment on mechanical and morphological properties of tropical wood polymer composites," *Mater. Des.* 33, 419-424. DOI: 10.1016/j.matdes.2011.04.044
- Salleh, F. M., Hassan, A., Yahya, R., Lafia-Araga, R. A., Azzahari, A. D., and Nazir, M. N. Z. M. (2014). "Improvement in the mechanical performance and interfacial behavior of kenaf fiber reinforced high density polyethylene composites by the addition of maleic anhydride grafted high density polyethylene," *J. Polym. Res.* 21, 439. DOI: 10.1007/s10965-014-0439-y
- Sánchez-Jiménez, P. E., Pérez-Maqueda, L. A., Perejón, A., and Criado, J. M. (2012). "Nanoclay nucleation effect in the thermal stabilization of a polymer nanocomposite: A kinetic mechanism change," *J. Phys. Chem. C* 116(21), 11797-11807. DOI: 10.1021/jp302466p
- Sasthiryar, S., Abdul Khalil, H. P. S., Bhat, A. H., Ahmad, Z. A., Islam, M. N., Zaidon, A., and Dungani, R. (2014). "Nanobioceramic composites: A study of mechanical, morphological, and thermal properties," *BioResources* 9(1), 861-871. DOI: 10.15376/biores.9.1.861-871
- Shahadat, M., Teng, T. T., Rafatullah, M., and Arshad, M. (2015). "Titanium-based nanocomposite materials: A review of recent advances and perspectives," *Colloid. Surface. B* 126, 121-137. DOI: 10.1016/j.colsurfb.2014.11.049
- Sharma, A. K., Chaudhary, G., Kaushal, I., Bhardwaj, U., and Mishra, A. (2015). "Studies on nanocomposites of polyaniline using different substrates," *Am. J. Polym. Sci.* 5(1A), 1-6. DOI: 10.5923/s.ajps.201501.01
- Shipp, D. A. (2011). "Polymer-layered silicate nanocomposites," in: *Comprehensive Nanoscience and Technology*, D. L. Andrews, G. D. Scholes, G. P. Wiederrecht (eds.), Academic Press, Cambridge, MA, USA, pp. 265-276. DOI: 10.1016/B978-0-12-374396-1.00058-1
- Siddique, S. F., Priyanka, S., and Nishanth, L. (2017). "Behavior of reinforced cement concrete beam with bamboo as partial replacement for reinforcement," *Int. J. Civ. Eng. Technol.* 8(9), 580-587.
- Silva, C. R., Lago, R. M., Veloso, H. S., and Patricio, P. S. O. (2018). "Use of amphiphilic composites based on clay/carbon nanofibers as fillers in UHMWPE," *J. Braz. Chem. Soc.* 29(2), 278-284. DOI: 10.21577/0103-5053.20170138

- Tao, Y. B., You, Y., and He, Y. L. (2016). "Lattice Boltzmann simulation on phase change heat transfer in metal foams/paraffin composite phase change material," *Appl. Therm. Eng.* 93, 476-485. DOI: 10.1016/j.applthermaleng.2015.10.016
- Thakur, V. K., Thakur, M. K., and Gupta, R. K. (2014). "Review: Raw natural fiber-based polymer composites," *Int. J. Polym. Anal. Charact.* 19(3), 256-271. DOI: 10.1080/1023666X.2014.880016
- Thomas, S., Kuruvilla, J., Malhotra, S. K., Goda, K., and Sreekala, M. S. (2012). *Polymer Composites Vol. 1*, Wiley-VCH, Weinheim, Germany. DOI: 10.1002/9783527645213
- Thostenson, E. T., Li, C., and Chou, T.-W. (2005). "Nanocomposites in context," *Compos. Sci. Technol.* 65(3-4), 491-516. DOI: 10.1016/j.compscitech.2004.11.003
- Varghese, A. M., and Mittal, V. (2018). "Polymer composites with functionalized natural fibers," in: *Biodegradable and Biocompatible Polymer Composites*, N. G. Shimpi (ed.), Woodhead Publishing, Cambridge, United Kingdom, pp. 157-186. DOI: 10.1016/B978-0-08-100970-3.00006-7
- Venkatesan, R., and Rajeswari, N. (2017). "TiO₂ nanoparticles/poly(butylene adipate-co-terephthalate) bionanocomposite films for packaging applications," *Polym. Adv. Technol.* 28(12), 1699-1706. DOI: 10.1002/pat.4042
- Wang, G., and Chen, F. (2017). "Development of bamboo fiber-based composites," in: *Advanced High Strength Natural Fibre Composites in Construction*, M. Fan, F. Fu (eds.), Woodhead Publishing, Cambridge, United Kingdom, pp. 235-255. DOI: 10.1016/B978-0-08-100411-1.00010-8
- Warman, R. D. (2014). "Global wood production from natural forests has peaked," *Biodivers. Conserv.* 23(5), 1063-1078. DOI: 10.1007/s10531-014-0633-6
- Xu, Y., Guo, Z., Fang, Z., Peng, M., and Shen, L. (2013). "Combination of double-modified clay and polypropylene-graft-maleic anhydride for the simultaneously improved thermal and mechanical properties of polypropylene," *J. Appl. Polym. Sci.* 128(1), 283-291. DOI: 10.1002/app.38178
- Yates, M. R., and Barlow, C. Y. (2013). "Life cycle assessments of biodegradable, commercial biopolymers - A critical review," *Resources, Conservation and Recycling* 78, 54-66. DOI: 10.1016/j.resconrec.2013.06.010
- Yu, Y.-L., Huang, X.-A., and Yu, W.-J. (2014). "High performance of bamboo-based fiber composites from long bamboo fiber bundles and phenolic resins," *J. Appl. Polym. Sci.* 131(12), Article ID 40371. DOI: 10.1002/app.40371
- Zhang, X., Wang, F., and Keer, L. M. (2015). "Influence of surface modification on the microstructure and thermo-mechanical properties of bamboo fibers," *Materials* 8(10), 6597-6608. DOI: 10.3390/ma8105327
- Zhu, Y., Romain, C., and Williams, C. K. (2016). "Sustainable polymers from renewable resources," *Nature* 540, 354-362. DOI: 10.1038/nature21001

Article submitted: July 7, 2019; Peer review completed: August 26, 2019; Revised version received: November 18, 2019; Accepted: November 19, 2019; Published: November 20, 2019.

DOI: 10.15376/biores.15.1.331-346